

Interface-Assisted Synthesis of Single-Crystalline ScF<sub>3</sub> MicrotubesLarisa B. Gulina,\*<sup>1</sup> Valeri P. Tolstoy, Yuri V. Petrov, and Denis V. Danilov

St. Petersburg State University, 7–9 Universitetskaya nab., St. Petersburg 199034, Russia

**ABSTRACT:** Scandium fluoride (ScF<sub>3</sub>) microtubes with nanoscale wall thickness were for the first time successfully synthesized by an interface-assisted technique at the surface of a scandium nitrate aqueous solution without the addition of any surfactant as a result of interaction with hydrofluoric acid from the gaseous phase in only 30 min. X-ray diffraction analysis, scanning electron microscopy, helium ionic microscopy, transmission electron microscopy (TEM), and high-resolution TEM (HRTEM) were used to examine the morphology and crystal structure of ScF<sub>3</sub> microtubes. The results show that the ScF<sub>3</sub> microtube is single-crystalline and has a hexagonal structure. A hypothetical model of thin-walled microtube formation is proposed.

The synthesis of inorganic nano- and microtubes is an important area of modern chemistry and materials science because of the great potential applications of such materials. Typically, such materials have high specific surface areas, which is important for catalyst and sorbent preparation. Moreover, single nano- or microstructures can be used in nano- and microdevices as individual components.<sup>1</sup> Various methods are used to obtain inorganic microtubes: hydrothermal synthesis,<sup>2</sup> rolled-up technology,<sup>3</sup> a template-assisted route,<sup>4</sup> vapor-phase deposition,<sup>5</sup> and crystallization from an aqueous solution.<sup>6</sup>

Scandium fluoride (ScF<sub>3</sub>) is a unique representative of a class of compounds with negative thermal expansion (NTE).<sup>7</sup> It can be present in composite materials with zero thermal expansion (ZTE),<sup>8</sup> can be used in optical and luminescent materials,<sup>9</sup> in catalysts,<sup>10</sup> and as a component of fluoride solid electrolytes.<sup>11</sup> To date, there have been no reports on the preparation of ScF<sub>3</sub> nano- or microtubes. Moreover, tubular structures of inorganic materials with NTE have not yet been demonstrated.

The aim of the present work is the synthesis of single-crystalline ScF<sub>3</sub> microtubes by a simple interface-assisted one-step method.

All of the chemicals were of analytical grade and were used as received without further purification. All of the aqueous solutions were prepared using Milli-Q high-purity water with a resistivity of more than 18 MΩ cm<sup>-1</sup>. The synthesis was carried out using the gas-solution interface technique (GSIT).<sup>12</sup> Earlier,<sup>13</sup> the synthesis of ScF<sub>3</sub> nanorods was carried out on the surface of a scandium chloride (ScCl<sub>3</sub>) solution with concentrations in the range of 0.01–0.10 M and pH values in the range of 1.0–3.0. In this work, a strongly acidic nitric acid (HNO<sub>3</sub>) solution of the 0.02 M scandium nitrate [Sc(NO<sub>3</sub>)<sub>3</sub>] salt was used as the reagent. In a typical procedure, scandium oxide (Sc<sub>2</sub>O<sub>3</sub>; 69 mg) was dissolved in 25 mL of a 1 M HNO<sub>3</sub> water solution. Then 3 mL of the Sc(NO<sub>3</sub>)<sub>3</sub> solution obtained was transferred into a flat beaker and put into a reactor. A vessel

with 3 mL of a 40% hydrofluoric acid (HF) aqueous solution, which was taken as a gaseous reagent, was placed near the scandium salt solution. All of the vessels and the reactor were made of Teflon. The scandium salt solution under steady-state conditions was exposed to gaseous HF for 20–60 min. After processing, a white film was obtained on the surface of the solution. It was washed several times with deionized water and dried at room temperature for 2 h.

The product was examined by X-ray diffraction (XRD) employed using a Rigaku “Miniflex II” diffractometer with Cu Kα radiation (λ = 1.5418 Å). Scanning electron microscopy (SEM) images were obtained by a Zeiss Merlin microscope equipped with an INCAx-act energy-dispersive X-ray analyzer (Oxford Instruments). A helium ionic microscopy (HeIM) study was performed by a Carl Zeiss Orion microscope using helium ions as a probe. Transmission electron microscopy (TEM), high-resolution TEM (HRTEM), and selected-area electron diffraction (SAED) measurements were taken using a Zeiss Libra 200 field-emission transmission electron microscope.

After a 60 min of synthesis, a discrete film is formed on the surface of the scandium salt solution; the film consists of 1D crystals with lengths of up to several micrometers (Figure 1a).

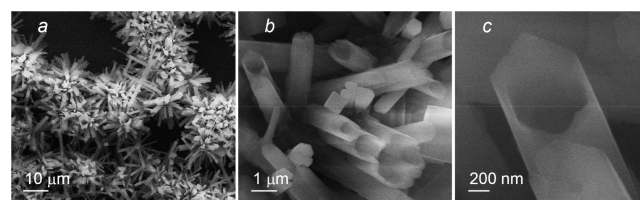


**Figure 1.** SEM images of ScF<sub>3</sub> microtubes: (a and b) overview images with different magnifications; (c) view of the open end of the single tube.

Most of the crystals are hollow microtubes with diameters of up to 1 μm and lengths of up to 5 μm (Figure 1b). It is very difficult to estimate the ratio of the tubes and rods in the sample considering that, in each part of the sample, we observed both hollow tubular structures and rodlike crystals whose orientation was such that we could not precisely define their structure. The thickness of the tube wall does not exceed 70 nm (Figure 1b,c).

It is clear (Figure 1c) that the tubes have a hexagonal structure. One can also note the presence of an insignificant amount of cubic crystals with a facet length of up to 400 nm (Figure 1b).

The results of the investigation of the synthesized sample by powder XRD are seen in Figure 2. They agree with the SEM data

**Received:** May 19, 2018

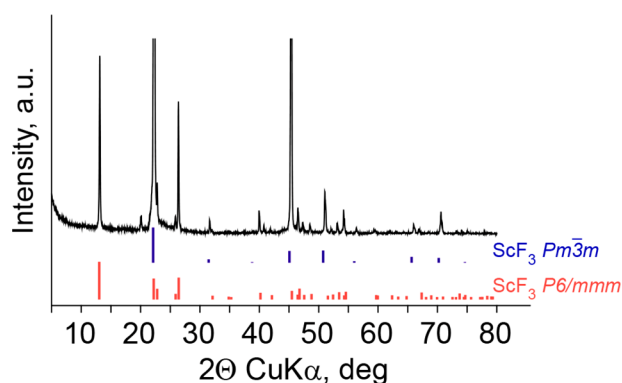


Figure 2. XRD pattern of the  $\text{ScF}_3$  sample.

and confirm the formation of a mixture of two  $\text{ScF}_3$  crystalline modifications, namely, of a cubic one with space group  $P\bar{m}3m$  (ICSD 77071)<sup>14</sup> and a hexagonal one with space group  $P6/mmm$ .<sup>15</sup>

Figure 3 shows a detailed morphology of the  $\text{ScF}_3$  microtubes. The HeIM images of the microtubes synthesized after 40 min of

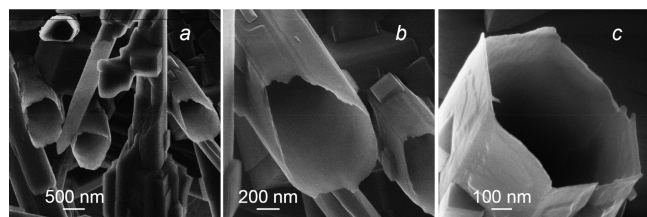


Figure 3. HeIM images of the  $\text{ScF}_3$  microtubes: (a) overview image; (b and c) views of the open ends of different tubes.

treatment are presented in Figure 3a–c. A typical open-ended crystal prismatic hexagon structure with well-defined crystallographic facets can clearly be seen. Thus, Figure 3b shows a tube with a diameter of about 850 nm and a wall thickness of 25 nm; Figure 3c shows a tube with a diameter of about 780 nm and a wall thickness of about 15 nm. It is obvious that the tube diameters are practically similar to the diameters of the tubes synthesized after 60 min of treatment (Figure 1), yet the wall thickness is smaller. One can also note the presence of cubic crystallites both as such and on the tube walls.

The results of TEM, HRTEM, and SAED measurements of the microtubes synthesized after 20 min of reaction are demonstrated in Figure 4. As is seen, the  $\text{ScF}_3$  microtube is of single-crystalline nature. SAED revealed that the characteristic orientation of the microtube corresponds to the  $c$ -axis direction (the zone axis is  $[001]$ ). It can be assumed from Figure 4b that

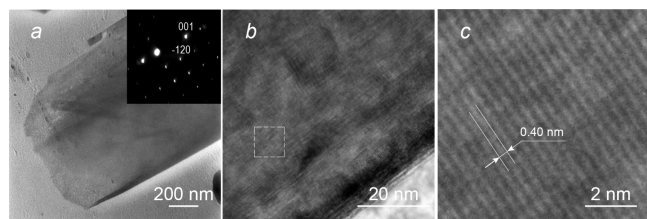


Figure 4. TEM and HRTEM images of the single  $\text{ScF}_3$  microtube: (a) overview image of a single tube and the corresponding SAED pattern in the inset; (b and c) HRTEM images of selected areas of a tube with different magnifications.

the thickness of the tube wall does not exceed 10 nm. The HRTEM image (Figure 4c) confirms the tube orientation along the  $c$  axis with a characteristic  $d_{(001)} = 0.40$  nm.

On the basis of the experimental data, one can propose the following model of  $\text{ScF}_3$  microtube formation at the interface between the  $\text{Sc}(\text{NO}_3)_3$  solution and gaseous HF. At the initial moment, free-floating hydrophobic nanocubes of  $\text{ScF}_3$  are formed on the surface of the solution; they can act as crystallization sites for further crystal growth of the microtubes, similar to the data of the work.<sup>16</sup> There are two possible causes for the growth of microtubular single-crystalline structures. First, a deficiency of scandium cations can be observed after formation of the cubic crystals in the microarea close to these crystals. It is known<sup>17</sup> that formation of the tubes arose from the low concentration of the precursor during deposition. In addition, the composition of the solution is a major factor in the formation of the tubular structures. To confirm this fact, we carried out interfacial reactions on the surfaces of (i) a highly acidic  $\text{ScCl}_3/\text{HNO}_3$  solution with a higher concentration of scandium salt (0.05 M) and (ii) a solution of  $\text{Sc}(\text{NO}_3)_3$  with the usual 0.02 M concentration and a higher pH of 2. In both cases, the formation of rod crystals of different sizes was observed, and no tubular structure was found. The role of the  $\text{HNO}_3$  action in the solution composition can consist of both the increasing of the solubility of the initial  $\text{ScF}_3$  crystals<sup>18</sup> and a competitive action of a large quantity of active ions in solution. At the second stage of the process, the growth rate is lower because of a smaller concentration of scandium cations. According to the experimental data, at this stage the thickness of the tube wall slowly increases because of the deposition of ions diffusing into the reaction zone from the solution. A hypothetical scheme of the tube formation process is presented in Figure 5. The hypothesis

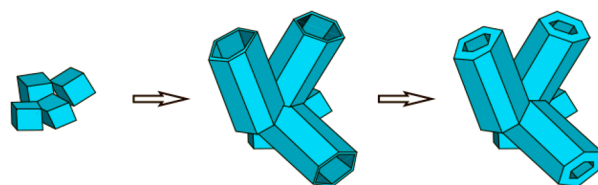


Figure 5. Hypothesized model of  $\text{ScF}_3$  microtube formation at the gas–solution interface.

of microtube formation is supported by the fact that, after 20 min of reaction, we observe microtubes with characteristic diameters and lengths. An increase in the reaction time from 20 to 60 min leads only to an increase in the wall thickness from 10 to 70 nm. Upon a further increase in the treatment time to 24 h, we did not observe any change in the tubular morphology. Apparently, this fact can indicate a natural end of the reaction as a result of the full deposition of poorly soluble  $\text{ScF}_3$ .

It is known<sup>15</sup> that both cubic and hexagonal polymorphs of  $\text{ScF}_3$  display strong NTE in a wide temperature range at normal pressure. The microtubes synthesized can be used not only in the design of materials with NTE or ZTE but also as a transparent optical array or as individual components in microelectronic devices, for example, to provide protection for highly sensitive units in microelectronic systems against thermal variation.

In conclusion,  $\text{ScF}_3$  nanowalled microtubes have been successfully synthesized by the GSIT route, based on the interface-assisted chemical reaction between gaseous HF and the surface of a  $\text{Sc}(\text{NO}_3)_3/\text{HNO}_3$  water solution without the

addition of any surfactant. The results of the investigation of the morphologies and crystal structures of the microtubes using XRD, SEM, HeIM, TEM, HRTEM, and SAED confirm that ScF<sub>3</sub> microtubes have a single-crystalline nature with hexagonal structure. Variation of the interaction time from 20 to 60 min is a major factor influencing the microtube wall thickness.

## AUTHOR INFORMATION

### Corresponding Author

\*E-mail: l.gulina@spbu.ru. Phone: +7(812)4284104.

### ORCID

Larisa B. Gulina: 0000-0002-1622-4311

### Author Contributions

All authors have given approval to the final version of the manuscript.

### Notes

The authors declare no competing financial interest.

## ACKNOWLEDGMENTS

We thank the Russian Science Foundation for financial support (Grant 16-13-10223) and the Research Park of St. Petersburg State University, Center of Nanotechnology and Centre for X-ray Diffraction Studies, for support with characterization of the crystals. We also thank Prof. A. Minchenkov for his assistance in the preparation of the paper.

## REFERENCES

- (1) Nuraeva, A.; Vasilev, S.; Vasileva, D.; Zelenovskiy, P.; Chezganov, D.; Esin, A.; Kopyl, S.; Romanyuk, K.; Shur, V. Y.; Kholkin, A. L. Evaporation-Driven Crystallization of Diphenylalanine Microtubes for Microelectronic Applications. *Cryst. Growth Des.* **2016**, *16*, 1472–1479.
- (2) (a) Tao, F.; Guan, M.; Zhou, Y.; Zhang, L.; Xu, Z.; Chen, J. Fabrication of Nickel Hydroxide Microtubes with Micro- and Nano-Scale Composite Structure and Improving Electrochemical Performance. *Cryst. Growth Des.* **2008**, *8*, 2157–2162. (b) Krasilin, A. A.; Gusarov, V. V. Control Over Morphology of Magnesium-Aluminum Hydrosilicate Nanoscrolls. *Russ. J. Appl. Chem.* **2015**, *88*, 1928–1935. (c) Zhuang, J.; Liang, L.; Sung, H. H. Y.; Yang, X.; Wu, M.; Williams, I. D.; Feng, S.; Su, Q. Controlled Hydrothermal Growth and Up-Conversion Emission of NaLnF<sub>4</sub> (Ln = Y, Dy–Yb). *Inorg. Chem.* **2007**, *46*, 5404–5410.
- (3) (a) Streubel, R.; Lee, J.; Makarov, D.; Im, M. Y.; Karnaushenko, D.; Han, L.; Schäfer, R.; Fischer, P.; Kim, S. K.; Schmidt, O. G. Magnetic Microstructure of Rolled-Up Single-Layer Ferromagnetic Nanomembranes. *Adv. Mater.* **2014**, *26*, 316–323. (b) Yin, Y.; Qiu, T.; Ma, L.; Lang, X.; Zhang, Y.; Huang, G.; Mei, Y.; Schmidt, O. G. Exploring Rolled-up Au–Ag Bimetallic Microtubes for Surface-Enhanced Raman Scattering Sensor. *J. Phys. Chem. C* **2012**, *116*, 25504–25508.
- (4) Mikhailov, V. I.; Krivoschapina, E. F.; Ryabkov, Y. I.; Krivoschapkin, P. V. Influence of the Electrokinetic Properties of Cellulose on the Morphology of Iron(III) Oxide upon Template Synthesis. *Glass Phys. Chem.* **2016**, *42*, 582–589.
- (5) Filippo, E.; Manno, D.; Serra, A. Characterization and Growth Mechanism of Selenium Microtubes Synthesized by a Vapor Phase Deposition Route. *Cryst. Growth Des.* **2010**, *10*, 4890–4897.
- (6) (a) Xin, Z.; Peng, J.; Wang, T.; Xue, B.; Kong, Y.; Li, L.; Wang, E. Keggin POM Microtubes: a Coincident Product of Crystal Growth and Species Transformation. *Inorg. Chem.* **2006**, *45*, 8856–8858. (b) Shen, Y.; Peng, J.; Zhang, H.; Yu, X.; Bond, A. M. Mo-Substituted Keggin Tungstosilicate Microtubes: Preparation and Characterization. *Inorg. Chem.* **2012**, *51*, 5146–5151.
- (7) (a) Greve, B. K.; Martin, K. L.; Lee, P. L.; Chupas, P. J.; Chapman, K. W.; Wilkinson, A. P. Pronounced Negative Thermal Expansion from a Simple Structure: Cubic ScF<sub>3</sub>. *J. Am. Chem. Soc.* **2010**, *132*, 15496–15498. (b) Hu, L.; Chen, J.; Fan, L.; Deng, J.; Yu, R.; Xing, X. Rapid Molten Salt Synthesis of Isotropic Negative Thermal Expansion ScF<sub>3</sub>. *J. Am. Ceram. Soc.* **2014**, *97*, 1009–1011.
- (8) (a) Hu, L.; Chen, J.; Fan, L.; Ren, Y.; Rong, Y.; Pan, Z.; Deng, J.; Yu, R.; Xing, X. Zero Thermal Expansion and Ferromagnetism in Cubic Sc<sub>1-x</sub>M<sub>x</sub>F<sub>3</sub> (M = Ga, Fe) over a Wide Temperature Range. *J. Am. Chem. Soc.* **2014**, *136*, 13566–13569. (b) Qin, F.; Chen, J.; Aydemir, U.; Sanson, A.; Wang, L.; Pan, Z.; Xu, J.; Sun, C.; Ren, Y.; Deng, J.; Yu, R.; Hu, L.; Snyder, G. J.; Xing, X. Isotropic Zero Thermal Expansion and Local Vibrational Dynamics in (Sc,Fe)F<sub>3</sub>. *Inorg. Chem.* **2017**, *56*, 10840–10843.
- (9) (a) Han, L.; Wang, Y.; Guo, L.; Zhao, L.; Tao, Y. Multifunctional ScF<sub>3</sub>:Ln<sup>3+</sup> (Ln = Tb, Eu, Yb, Er, Tm and Ho) Nano/Microcrystals: Hydrothermal/Solvothermal synthesis, Electronic Structure, Magnetism and Tunable Luminescence Properties. *Nanoscale* **2014**, *6*, 5907–5917. (b) Pei, W.-B.; Wang, L.; Wu, J.; Chen, B.; Wei, W.; Lau, R.; Huang, L.; Huang, W. Controlled Synthesis of Uniform Na<sub>x</sub>ScF<sub>3+x</sub> Nanopolyhedrons, Nanoplates, Nanorods, and Nanospheres Using Solvents. *Cryst. Growth Des.* **2015**, *15*, 2988–2993.
- (10) Kokubo, M.; Kobayashi, S. Scandium(III) Fluoride as a Novel Catalyst for Hydroxymethylation of Dimethylsilyl Enolates in Aqueous Media. *Synlett* **2008**, *2008* (10), 1562–1564.
- (11) (a) Trnovcová, V.; Fedorov, P. P.; Furár, I. Fluoride Solid Electrolytes. *Russ. J. Electrochem.* **2009**, *45*, 630–639. (b) Trnovcová, V.; Fedorov, P. P.; Buchinskaya, I. I.; Smatko, V.; Hanic, F. Fast Ionic Conductivity of PbF<sub>2</sub>:MF<sub>2</sub> (M = Mg, Ba, Cd) and PbF<sub>2</sub>:ScF<sub>3</sub> Single Crystals and Composites. *Solid State Ionics* **1999**, *119*, 181–189.
- (12) (a) Gulina, L. B.; Tolstoy, V. P.; Kasatkin, I. A.; Petrov, Y. V. Facile Synthesis of LaF<sub>3</sub> Strained 2D Nanoparticles and Microtubes at Solution-Gas Interface. *J. Fluorine Chem.* **2015**, *180*, 117–121. (b) Tolstoy, V. P.; Gulina, L. B. Synthesis of Birnessite Structure Layers at the Solution-Air Interface and the Formation of Microtubules from them. *Langmuir* **2014**, *30*, 8366–8372.
- (13) Gulina, L. B.; Tolstoy, V. P.; Kasatkin, I. A.; Murin, I. V. Facile Synthesis of Scandium Fluoride Oriented Single-Crystalline Rods and Urchin-Like Structures by a Gas-Solution Interface Technique. *CrystEngComm* **2017**, *19*, 5412–5416.
- (14) Fedorov, P. P.; Trnovcová, V.; Kocherba, G. I.; Sobolev, B. P. Ionic-Conductivity and Dielectric-Relaxation of Scandium Fluoride. *Kristallografiya* **1995**, *40*, 716–720.
- (15) Kasatkin, I. A.; Gulina, L. B.; Platonova, N. V.; Tolstoy, V. P.; Murin, I. V. Strong Negative Thermal Expansion in the Hexagonal Polymorph of ScF<sub>3</sub>. *CrystEngComm* **2018**, *20*, 2768–2771.
- (16) Fan, F.-R.; Ding, Y.; Liu, D.-Y.; Tian, Z.-Q.; Wang, Z. L. Facet-Selective Epitaxial Growth of Heterogeneous Nanostructures of Semiconductor and Metal: ZnO Nanorods on Ag Nanocrystals. *J. Am. Chem. Soc.* **2009**, *131*, 12036–12037.
- (17) (a) Yu, L.; Zhang, G.; Li, S.; Xi, Z.; Guo, D. Fabrication of Arrays of Zinc Oxide Nanorods and Nanotubes in Aqueous Solution under an External Voltage. *J. Cryst. Growth* **2007**, *299*, 184–188. (b) Xu, S.; Wang, Z. L. One-Dimensional ZnO Nanostructures: Solution Growth and Functional Properties. *Nano Res.* **2011**, *4*, 1013–1098.
- (18) Amano, O.; Sasahira, A.; Kani, Y.; Hoshino, K.; Aoi, M.; Kawamura, F. Solubility of Lanthanide Fluorides in Nitric Acid Solution in the Dissolution Process of FLUOREX Reprocessing System. *J. Nucl. Sci. Technol.* **2004**, *41*, 55–60.